Scientia Iranica D (2021) 28(3), 1669–1684

Sharif University of Technology
Scientia Iranica
Transactions D: Computer Science & Engineering and Electrical Engineering
http://scientiairanica.sharif.edu

Effect of diluted connectivities on cluster synchronization of adaptively coupled oscillator networks

S. Vock[a], R. Berner[a,b], S. Yanchuk[b], and E. Schöll[a,c,d,*]

a. *Institute of Theoretical Physics, Technische Universität Berlin, Hardenbergstraβe 36, 10623 Berlin, Germany.*
b. *Institute of Mathematics, Technische Universität Berlin, Straβe des 17. Juni 136, 10623 Berlin, Germany.*
c. *Bernstein Center for Computational Neuroscience Berlin, Humboldt-Universität, Philippstraβe 13, 10115 Berlin, Germany.*
d. *Potsdam Institute for Climate Impact Research, Telegrafenberg A 31, 14473 Potsdam, Germany.*

Received 14 January 2021; received in revised form 16 April 2021; accepted 24 May 2021

KEYWORDS
Master stability;
Phase oscillators;
Adaptive networks;
Complex networks;
Cluster states;
Desynchronization;
Synaptic plasticity.

Abstract. Synchronization of networks of oscillatory units is an emergent phenomenon that has been observed in a variety of systems from power grids to ensembles of nerve cells. Many real-world networks are characterized by adaptive properties; in other words, depending on the dynamical states of the system, their connectivity changes with time. Networks of adaptively coupled oscillators exhibit different synchronization phenomena such as hierarchical multifrequency clusters, traveling waves, or chimera states. While these self-organized patterns have been previously studied in all-to-all coupled networks, the present study further investigated more complex networks by analyzing the effect of random network topologies with different dilution degrees of connectivity. The numerical and analytical approaches were employed to investigate the robustness of multi-cluster states on networks of adaptively coupled Kuramoto-Sakaguchi oscillators against random dilution of the underlying network topology. In addition, a master stability approach was used in adaptive networks to highlight the interplay between adaptivity and topology. Through this approach, the robustness of multifrequency cluster states to diluted connectivities can be illustrated.

1. Introduction

In general terms, a complex dynamical network is a set of dynamical units (nodes) with connections among them (links), representing a relation or interaction among the individual elements. In nature as well as in technology, complex dynamical networks provide a framework with a broad range of applications in physics, chemistry, biology, neuroscience, economy, social science, etc. [1,2].

Collective behavior of dynamical networks is an emergent phenomenon of spontaneously ordered dynamics. One example of their particular significance is synchronization [3–7]. First recognized by Huygens in the 17th century [8], synchronization phenomena in coupled oscillators are of great significance in science, nature, engineering, and social life. Depending on the dynamical properties of a system, diverse synchronization patterns of varying complexity such as complete synchronization [9,10], cluster synchronization [11–15], and different forms of partial synchronization [16–

*. *Corresponding author.*
E-mail address: schoell@physik.tu-berlin.de (E. Schöll)

doi: 10.24200/sci.2021.57526.5284

28] have been observed. Synchronization patterns are believed to play a key role in neural networks, e.g., in the context of cognition and learning [29–31], pathological conditions such as Parkinson's disease [32–35], or epilepsy [36–43].

A central question in the study of synchronization in complex networks is whether or not such behavior is stable. In this regard, the master stability approach is a powerful analytic framework used to study the stability of synchronized states [44]. Since its introduction, this approach has been extended to different types of networks such as multilayer networks [45,46], networks with time-delays [13,47–57], hypernetworks [58,59], and very recently, adaptive networks [60]. The master stability approach allows for separating the effects of local node dynamics from those of the network topology. This approach can be used to draw general conclusions on the stability of dynamical systems by analyzing the eigenvalues of the network connectivity matrix.

A majority of the previous studies have analyzed the dynamical processes occurring in static networks, describing the fixed interaction structures with no change during time. However, real-world networks often change in time, adapting their structure in response to the network state [61–63]. This type of network called adaptive or co-evolutionary combines the topological evolution of the network with dynamics on the network nodes. This behavior is observed in a number of real-world applications. For instance, power grids and traffic networks continuously change to meet the evolving requirements of society. Further, adaptive behavior is of great significance in neural networks, i.e., networks of individual neurons connected by synapses that pass electrical or chemical signals among them. As shown, the coupling weights among the individual neurons may be potentiated or depressed, depending on the order of the spike times of post- and pre-synaptic neurons [64–66]. This mechanism called *spike timing-dependent plasticity* is believed to play an important role in temporal coding of information in the brain [67].

In this study, the robustness of multi-cluster states was investigated in the networks of adaptively coupled Kuramoto-Sakaguchi oscillators against random dilution of the underlying network topology. By randomly and successively deleting links, we observe a linear dependence of the cluster frequencies on the relative number of deleted links. This linear dependence can be elaborated by a suitable approximation of the frequencies of oscillators. In addition, it was numerically shown that the shape of a multi-cluster state was preserved on networks of different sparsity, ranging from fully coupled to almost uncoupled topologies. Further, it was found that the observed multi-cluster states were multi-stable, indicating that different multi-clusters might emerge from different initial conditions. The master stability approach was used for adaptive networks to present the effects induced by changes of the network topology on the desynchronization of the phase synchronized state. As shown, the resulting desynchronization had strong implications for the emergence of multi-cluster states.

The present study is organized as follows. In Section 2, the model used in this study is introduced. In Section 3, the emergence and structural formations of multi-frequency-cluster states are discussed. In Section 4, the effect of random dilution of links in the connectivity structure on multi-cluster states is investigated by applying a suitable randomization process on the network connectivity. In Section 5, the master stability approach is used for adaptive networks to investigate the interplay between the nodal dynamics, adaptivity, and a complex connectivity structure. Finally, in Section 6, the obtained results are given to further elaborate a desynchronization transition by changes in the network topology.

2. Model

One successful approach to studying the different aspects of synchronization phenomena in networks of coupled oscillators is offered by the paradigmatic Kuramoto model [9]. We consider a network of Kuramoto-Sakaguchi type phase oscillators with adaptive coupling weights [63,68,69]:

$$\dot{\phi}_i = \omega - \sigma \sum_{j=1}^{N} a_{ij}\kappa_{ij} \sin(\phi_i - \phi_j + \alpha), \tag{1}$$

$$\dot{\kappa}_{ij} = -\epsilon(\kappa_{ij} + a_{ij} \sin(\phi_i - \phi_j + \beta)), \tag{2}$$

where $\phi_i(t) \in [0, 2\pi)$ describes the phase of oscillator $i \in \{1, ..., N\}$ and $\kappa_{ij}(t) \in [-1, 1]$ denotes the coupling strength from oscillator j to i. The connectivity structure is composed of elements $a_{ij} \in \{0, 1\}$ of the adjacency matrix A which is independent of time. Note that self-coupling does not affect the relative dynamics, which is the reason why the N diagonal elements a_{ii} are set to zero in all our simulations. Eq. (1) describes a network of Kuramoto-Sakaguchi type phase oscillators with a diffusive coupling kernel $\sin(\phi_i - \phi_j + \alpha)$ scaled by the overall coupling strength σ, where ω is the intrinsic frequency. The parameter α can be considered as the phase lag of the interactions among the oscillators [70], which is even related to a synaptic propagation delay [71]. Eq. (2) describes the dynamics of the coupling weights κ_{ij} and $\epsilon \ll 1$ is the time-scale separation parameter. We define the adaptation function as $-\sin(\phi_i - \phi_j + \beta)$, where β is a control parameter, enabling us to implement different plasticity rules that would occur in neural networks (see Figure 1). For instance, setting $\beta = -\pi/2$ (Figure 1(a)) would lead to

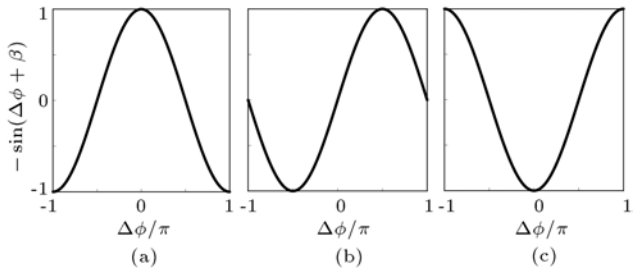

Figure 1. The adaptation function $-\sin(\Delta\phi+\beta)$ used in System (1)-(2) for the parameter values: (a) $\beta=-\pi/2$ (Hebbian), (b) $\beta=0$ (causal, effectively similar to spike timing-dependent plasticity), and (c) $\beta=\pi/2$ (anti-Hebbian).

the adaptation function corresponding to a Hebbian-like rule. In this case, the adaptation function is positive and causes an increase in the synaptic weights if the phase differences of the post- and pre-synaptic neurons are close to each other, $|\Delta\phi|<\pi/2$ where $\Delta\phi=\phi_i-\phi_j$.

The synchrony of the oscillators at a given time t is typically quantified by the Kuramoto-Daido order parameter [9,72]. The complex nth order parameter for the state $\phi(t)=(\phi_1(t),...,\phi_N(t))^T$ is defined as:

$$Z_n(\phi(t))=R_n(t)e^{i\psi_n(t)}=\frac{1}{N}\sum_{j=1}^{N}e^{in\phi_j(t)}, \tag{3}$$

where $\psi_n(t)$ is the collective mean phase of the population, and the modulus $R_n(t)$ is given by the absolute value $R_n(t)=|(1/N)\sum_{j=1}^{N}e^{in\phi_j(t)}|$. The quantity $n\in\mathbb{N}$ is also referred to as the nth moment of the order parameter. Here, $i=\sqrt{-1}$ denotes the imaginary unit. The first-order parameter Z_1 can be regarded as the centroid of the N phases of the oscillators represented on the unit circle, i.e., on the complex plane [73]. In the case of in-phase synchronization, i.e., $\phi=(a,...,a)^T$ for some $a\in[0,2\pi]$, the modulus $R_n=1$. If $R_n=0$, the oscillators are regarded as incoherent in terms of the nth moment. This property can be used to distinguish between the particular types of coherence in terms of certain discrete phase distributions (see Section 3).

3. Multicluster states in adaptive networks of phase oscillators

System (1)-(2) generalizes Kuramoto-Sakaguchi type systems with fixed value of κ_{ij}. Recently, this model has drawn considerable attention, e.g., in synaptic plasticity and learning [62,68,74–78], multistability [79–81], topological characteristics [82,83], delay [84], hierarchical synchronization patterns [63,85], and multiplex networks [86]. In this section, we briefly summarize the findings that were already reported in [63,69,87] and show different types of multicluster states that emerge on an all-to-all coupled base topology $a_{ij}=1(i\neq j)$, starting from random initial conditions ($\phi_i\in[0,2\pi)$, $\kappa_{ij}\in[-1,1]$ for all $i,j=1,...,N$). These states are characterized by strongly coupled oscillators within each cluster but weak couplings between the clusters. While all oscillators in one cluster share a common frequency, the frequencies between the clusters are different.

In a multicluster state, the coupling weight matrix with elements κ_{ij} can be divided into $M\in\mathbb{N}$ blocks, called clusters, each containing a number N_μ ($\mu=1,...,M$) of frequency synchronized oscillators. The entries of this coupling weight matrix are denoted by $\kappa_{ij,\mu\nu}$, referring to the coupling weight from the jth oscillator in the νth cluster to the ith oscillator in the μth cluster. For the temporal behavior of an oscillator in an M-cluster state, the following form is taken into consideration:

$$\phi_{i,\mu}(t)=\Omega_\mu t+a_{i,\mu}+s_{i,\mu}(t), \tag{4}$$

where $\phi_{i,\mu}$ denotes the phase of oscillator i inside the cluster μ, Ω_μ is the collective frequency of the cluster, $a_{i,\mu}\in[0,2\pi)$ are the phase lags, and function $s_{i,\mu}(t)$ is the bounded function resulting from the interaction among the clusters.

Despite the constant frequencies within a cluster, we can differentiate between three types of multiclusters, depending on the oscillator phases [69,87]. The first type is called *splay-type* multicluster (Figure 2(a), (c), and (e)). In this case, the coupling weights $\kappa_{ij,\mu\nu}$ are either constant or changing periodically in time, depending on whether the oscillators $\phi_{i,\mu}$ and $\phi_{j,\nu}$ belong to either the same ($\mu=\nu$) or a different ($\mu\neq\nu$) cluster, respectively. The amplitude of the coupling weights depends on the difference in the frequency of the clusters, where the greater the frequency difference, the smaller the amplitude. The classification into three strongly coupled clusters as well as the hierarchical structure in the cluster size is illustrated in Figure 2(a), (c), and (e). The oscillators are distributed based on their phases on the unit circle such that the phases of each splay-type cluster fulfill the condition $R_2(a_\mu)=0$ for $\mu=1,2,3$ (cf., Eq. (3)).

Figure 2(b), (d), and (f) show another possible type of multicluster. Here, the oscillators of each cluster possess the phase $a_{i,\mu}=a_\mu$ or the antipodal phase $a_{i,\mu}=a_\mu+\pi$, such that $2a_{i,\mu}=2a_\mu$ for all $i=1,...,N_\mu$. Therefore, we call these states *antipodal-type* multi-cluster. In contrast to splay states, the phase distribution of this type of state fulfills $R_2(a_\mu)=1$, where $\mu=1,2$. Note that in-phase synchronous states belong to this type of clusters.

The third possible type of multi-clusters combines the previous two types, where the cluster can be either of splay- or antipodal-type. These states are called

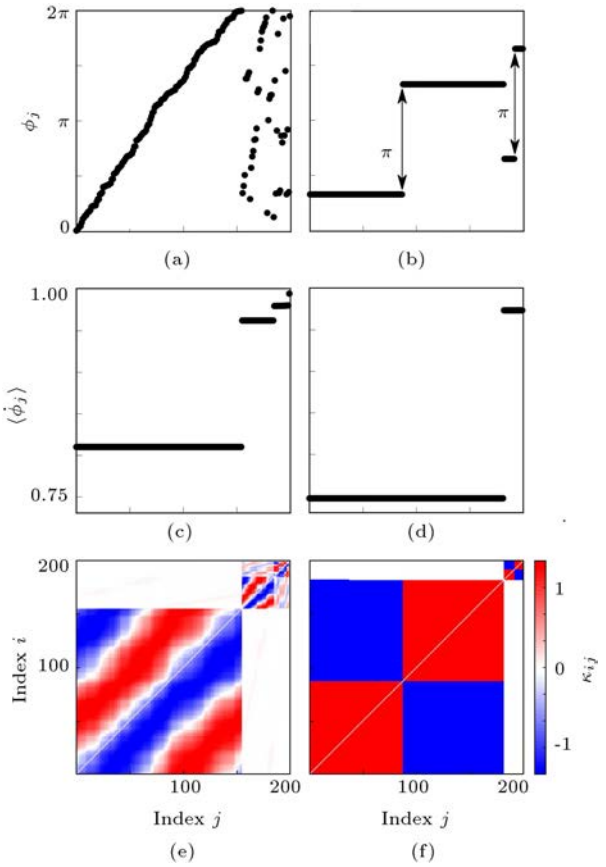

Figure 2. Two types of multicluster states in a network of $N = 200$ adaptively coupled phase oscillators (Eqs. (1) and (2)) with different parameter values α and β. (a) and (b): Snapshots of the phases ϕ_j at $t = 20000$; (c) and (d): mean frequencies $\langle\dot{\phi}_j\rangle = (\phi(t_0 + T) - \phi(t_0))/T$ with $t_0 = 10000$, $T = 10000$; (e) and (f): snapshots of the coupling matrices κ_{ij} at $t = 20000$. In (a), (c), and (e), a splay-type multicluster for $\alpha = 0.2\pi$, $\beta = 0.15\pi$ and in (b), (d), and (f) an antipodal-type multicluster with $\alpha = 0.2\pi$, $\beta = -0.6\pi$ are presented. Other parameters are $\epsilon = 0.01$, $\omega = 1$, $\sigma = 1/N$.

mixed-type multi-clusters. For more details, refer to [69,87].

The appearance of multi cluster states suggests that certain one-cluster states serve as building blocks for more complex multi-cluster states. Formally, a one-cluster state is a frequency-synchronized group of phase oscillators described by:

$$\phi_i = \Omega t + a_i,$$

with collective frequency Ω, relative phase shifts $a_i \in [0, 2\pi)$, and $i = 1, ..., N$. Figure 3 shows the coupling matrices κ_{ij} of all three possible one-cluster states on an all-to-all network of adaptively coupled phase oscillators (1) and (2). Already mentioned above, the first two types, i.e., the splay clusters and antipodal clusters, serve as building blocks for multi-cluster states. The third type, shown in Figure 3(c), is called the double-antipodal state. It consists of two groups of antipodal phase oscillators with a fixed phase lag between them. In contrast to splay- and antipodal clusters, double-antipodal states are unstable for the whole range of parameters; therefore, they are unlikely to be found as building blocks for multi-cluster states.

4. Desynchronization of multiclusters by random dilution of network connections

Section 3 discussed the generic appearance of the multi-cluster states in System (1)-(2) on an all-to-all coupled network. Based on the phase relations of the oscillators within the clusters, we distinguished between splay- and antipodal multi-clusters. It was also shown that the oscillators could form groups of strongly connected units, where the interaction between the groups was weaker than that within the groups. This section investigates the robustness of multi-cluster states against the random dilution of the underlying network topology.

This study took into consideration a network of $N = 100$ adaptively coupled phase oscillators, described by Eqs. (1) and (2). The parameters $\alpha = 0.3$ and $\beta = -0.53$ were then fixed such that a multi-cluster state emerged from random initial conditions for an all-to-all coupled network structure. In order to implement the dilution of links, Q links ($Q \leq (N-1)N$) were randomly and successively deleted by choosing a set of Q indices (ij) randomly corresponding to the existing links in the adjacency matrix, i.e., $a_{ij} = 1$. These links are then removed, i.e., we set $a_{ij} = 0$. The degree of dilution, i.e., the ratio of deleted links, is defined as $q = Q/(N(N-1))$.

Then, two different numerical approaches were utilized to study the effects of dilution: (I) System (1)-(2) was numerically solved for 11000 time units and q successively increased in each simulation run, where the final multi-cluster state for $q = 0$ was set as the initial condition for all the following simulations. This approach was used to investigate the robustness of a known multi-cluster state against random dilution of links. (II) Then, a set of 100 different random initial conditions was fixed. For each q, the system dynamics was simulated for all 100 initial conditions and 11000 time units.

Figure 4 depicts three resulting states of System (1)-(2), obtained by the numerical simulations mentioned above. The coupling weights κ_{ij} are shown together with their corresponding mean frequencies $\langle\dot{\phi}_j\rangle = (\phi_i(t_0 + T) - \phi_i(t_0))/T$ for different values of q. Here, $t_0 = 10000$ and $T = 1000$ were chosen. In addition, the phases ϕ_j of the oscillators within the biggest cluster are represented on the unit circle. In the case of a fully coupled network ($q = 0$, Figure 4(a)), an antipodal-type multi-cluster state emerges, consisting

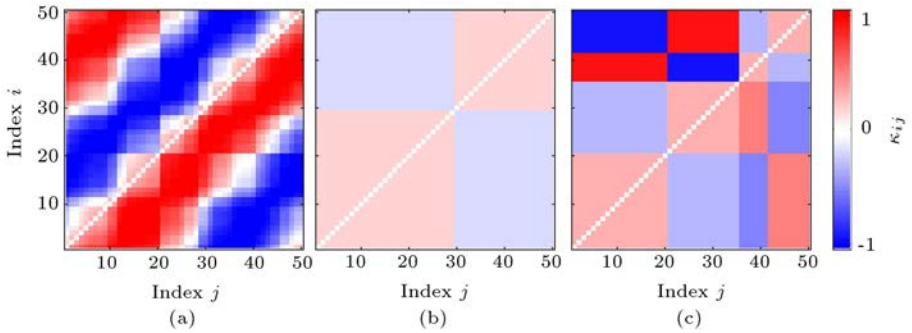

Figure 3. Illustration of the coupling weights κ_{ij} for all three existing types of one-cluster states in a network of $N = 50$ adaptively coupled phase oscillators (Eqs. (1) and (2)): (a) Splay state with $\alpha = 0.3\pi$, $\beta = 0.1\pi$, (b) antipodal state with $\alpha = 0.2\pi$, $\beta = -0.95\pi$, and (c) double-antipodal state with $\alpha = 0.3\pi$, $\beta = -0.15\pi$. Other parameters are $\epsilon = 0.01$, $\sigma = 1/N$. Adapted from [87].

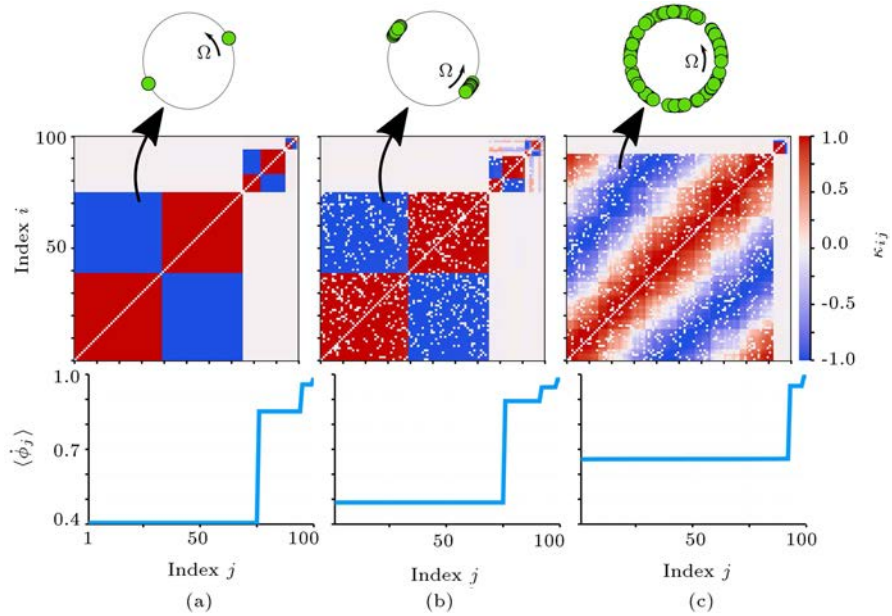

Figure 4. Three multicluster states in a network of adaptively coupled phase oscillators (Eqs. (1) and (2)) for different ratios of the deleted links q. At the bottom and middle panels, the mean frequencies $\langle\dot{\phi}_j\rangle = (\phi(t_0 + T) - \phi(t_0))/T$ with $t_0 = 10000$, $T = 1000$ and snapshots of the coupling weights κ_{ij} at $t = 11000$ are shown, respectively. The phases of the oscillators within the biggest cluster at $t = 11000$ represented on the unit circle are shown at the top panel: (a) $q = 0$, (b) and (c) $q = 0.13$ (different initial conditions: (b) multicluster state of panel and (a) and (c) random initial conditions). Other parameters are $N = 100$, $\epsilon = 0.01$, $\omega = 1$, $\alpha = 0.3\pi$, $\beta = -0.53\pi$, $\sigma = 1/N$.

of three groups. The average frequencies of the oscillators within each cluster are constant, as described in Section 3. Moreover, the oscillator phases within each cluster possess the phase difference of either 0 or π. Hence, the clusters are of the antipodal type. The smaller clusters possess a mean frequency closer to the natural frequency $\omega = 1$ due to their smaller size.

Figure 4(b) and (c) depict two possible states on networks with a dilution degree (ratio of deleted links) of $q = 0.13$, where the initial conditions were chosen as the multi-cluster state of Figure 4(a) in panel (b) and as random initial conditions in panel (c). Of note, the white dots in the coupling matrix represent the deleted links. The simulations showed that despite the missing links, the oscillators could still organize themselves in multi-clusters. The antipodal-type multi-cluster in Figure 4(b) has a similar shape as the multi-clusters previously observed. However, in the case of missing links, the phases ϕ_i within the clusters slightly spread out in order to compensate for the heterogeneity in the network topology. The splay-type cluster in Figure 4(c) is a different type of stable state that can emerge in System (1)-(2) for $q = 0.13$. Note that in Figure 4(b) and (c), the same parameter values are used, indicating that different types of multi-cluster patterns may emerge from random initial conditions. Therefore, multiclusters may exhibit multistability. In order to further investigate the robustness of multi-

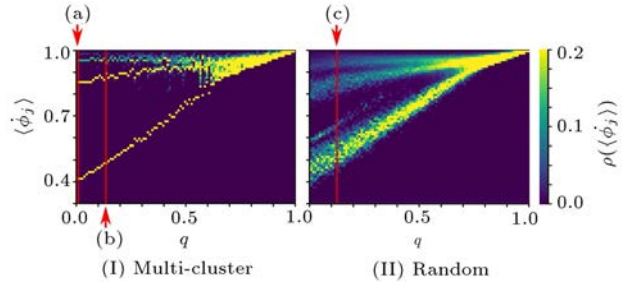

Figure 5. The robustness of multicluster states against a random dilution of links. Collective mean frequencies $\langle\dot{\phi}_j\rangle$ vs the ratio of deleted links q in a network of adaptively coupled phase oscillators (Eqs. (1) and (2)). (I) Distribution of the mean frequencies $\langle\dot{\phi}_j\rangle$, where the multicluster state obtained at $q = 0$ serves as the initial condition for all simulations with $q > 0$ and (II) distribution of mean frequencies averaged over 100 realizations of random initial conditions for each q. The red lines (a)–(c) mark the states shown in Figure 4. Note $\langle\dot{\phi}_j\rangle = (\phi_j(t_0 + T) - \phi_j(t_0))/T$, where $t_0 = 10000$ and $T = 1000$. Parameters: $N = 100$, $\epsilon = 0.01$, $\omega = 1$, $\alpha = 0.3\pi$, $\beta = -0.53\pi$, $\sigma = 1/N$.

clusters against dilution of the connectivities, Figure 5 presents the distribution ρ (color coded) of the mean frequencies $\langle\dot{\phi}_j\rangle$ of the oscillators versus the fraction of deleted links q. These results were obtained by applying two numerical approaches described above. Figure 5(I) presents the mean frequencies corresponding to the numerical procedure (I) where the multi-cluster state depicted in Figure 4(a) is set as an initial condition. Of note, the data used for each step of q is an average of all N oscillators. For a wide range of q, three distinct clusters are visible. For large values of q, where the network becomes sparse, the frequency clusters are not clearly separated. The qualitative shape of the initial multi-cluster state is preserved on the networks with different degrees of dilution, ranging from fully-coupled to almost uncoupled topologies. The number of clusters remains the same on networks with varying numbers of links; however, the collective mean frequencies of the oscillators adapt to the changes in the coupling topology in a linear relation with q.

The linear dependence of the cluster frequencies on the relative number of deleted links q can be explained as follows. For the increasing dilution q, each link is subject to an equal cut-off probability. Therefore, on average, there are $(1 - q)N_\mu(N_\mu - 1)$ links in each cluster. Furthermore, assuming that $\epsilon \ll 1$, the collective frequency of each cluster can be roughly approximated up to zeroth order ϵ by $\Omega_\mu \approx \omega + \sigma \sum_{j=1}^{N_\mu} a_{ij,\mu\mu} \sin(a_{i,\mu} - a_{j,\mu} + \beta) \sin(a_{i,\mu} - a_{j,\mu} + \alpha)$ [69]. Consider an approximately antipodal cluster, $a_{i,\mu} - a_{j,\mu} \approx 0$ or π. Then, $\Omega_\mu \approx \omega + \sigma \sin(\beta) \sin(\alpha) r_{i,\mu}$ where $r_{i,\mu} = \sum_{j=1}^{N_\mu} a_{ij,\mu\mu}$ is the ith row sum restricted to the μth cluster. By averaging over $i = 1, ..., N_\mu$, we end up with the approximation:

$$\Omega_\mu \approx \omega + \sigma(1 - q)(N_\mu - 1) \sin(\beta) \sin(\alpha). \quad (5)$$

The latter expression explains the linear dependence of the cluster frequency on the ratio of the deleted links. Furthermore, Eq. (5) shows that the slope of the linear relation depends on the cluster size. This finding is in agreement with that in Figure 5(I). Of note, splay clusters can be treated similarly. Figure 5(II) illustrates the distribution of collective mean frequencies versus q for random initial conditions according to the numerical procedure (II). Here, the data for each step of q is an average of 100 numerical runs. In this respect, the color code represents the fraction of oscillators that lie in the corresponding frequency band. For a wide range of q, the frequencies roughly show three maxima of $\rho(\langle\dot{\phi}_j\rangle)$, indicating three-cluster states (see the Appendix as an example). Further, two-cluster states of splay type, corresponding to the fourth smaller maximum of $\rho(\langle\dot{\phi}_j\rangle)$, were observed, being located slightly above the largest maximum and it would vanish in case $q > 0.4$. At the increasing values of q, the overall frequencies increased linearly as well and eventually converged on $\langle\dot{\phi}_j\rangle|_{q=1} = 1$. In this case, all nodes are uncoupled, oscillating with their natural frequency of $\Omega = 1$. These results can be compared with those in Reference [88], where the dynamical states on networks of adaptively coupled phase oscillators are studied in the (α, β) parameter space for different degrees of network dilution. As shown, splay- and antipodal-type clusters emerge in the corresponding region of the parameter space for all-to-all coupled networks. For decreasing numbers of links, i.e., increasing q, the network first loses its ability to reach the splay-type states and subsequently, fails to synchronize. These findings suggest that the fourth maximum in Figure 5(II) exists due to the presence of splay-type multi-clusters since it vanishes for $q > 0.4$.

The multi-cluster states described in Figure 5(I) are visualized by showing the corresponding snapshots of the coupling matrices κ_{ij} in Figure 6. As observed, the multi-cluster state at $q = 0$ was chosen as the initial condition for all simulations with $q > 0$. In agreement with our prior observations, three clusters are visible for densely connected networks. For increasing value of q, which is indicative of sparser networks, the frequency clusters dissolve in a hierarchical manner, where clusters consisting of fewer oscillators vanish prior to those containing a large number of oscillators. Further, it was observed that dissolution of a cluster started with uncoupling of the single oscillators from the cluster and a continuous decrease in the cluster size. This process continues until the cluster vanishes. A similar plot corresponding to Figure 5(II) with random

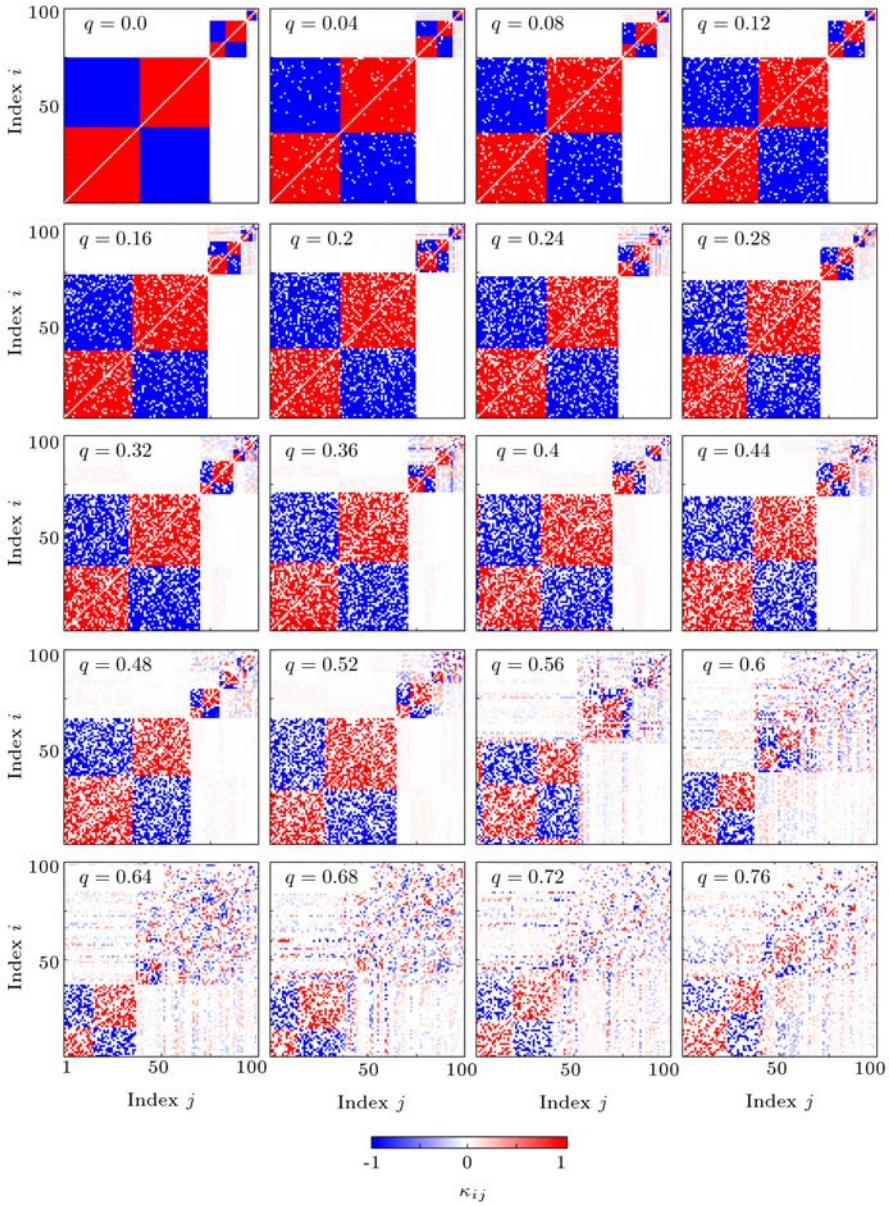

Figure 6. Effects of the successive dilution of links on a given multicluster state. Multicluster states in a network of adaptively coupled phase oscillators (Eqs. (1) and (2)) with a decreasing ratio of randomly deleted links $q = Q/(N(N-1))$. The multicluster state at $q = 0$ is used as the initial condition for all simulations with $q > 0$. Snapshots of the coupling matrices κ_{ij} at $t = 11000$ for different values of q are presented. In each panel, the oscillators are ordered according to their mean frequency and their phases. Parameters include $\alpha = 0.3\pi$, $\beta = -0.53\pi$, $\omega = 1$, $\epsilon = 0.01$, $\sigma = 1/N$, and $N = 100$.

initial conditions can be found in the Appendix. In this section, it is shown that random dilution of the network topology will desynchronize the multi-clusters. As observed, System (1)–(2) preserves the qualitative shape of the multi-cluster states on random networks of different sparsity. Hence, multi-clusters are robust against topological perturbations. Further, System (1)–(2) possesses a high degree of multistability for diluted network topologies. In the following section, the stability of the synchronized states is investigated using master stability function for networks with adaptive couplings [60]. Given this, it was suggested that the presence of adaptive couplings could affect the stability of System (1)–(2). Further, destabilization of the phase-synchronized state has implications for the emergence of multi-cluster states.

5. Master stability function for adaptive phase oscillator networks

In the previous section, desynchronization of multi-cluster states for a decreasing number of links was discussed. It was also shown that System (1)–(2) retained the ability to form strongly coupled groups

of oscillators in random initial conditions on networks with an increasing degree of dilution; however, the fraction of desynchronized oscillators increased in sparse networks. Since the individual clusters in a multi-cluster state are effectively uncoupled from each other, the stability of these strongly coupled subnetworks may play a significant role in the stability of multi-cluster states.

This section as well as the next section aim to gain analytic insights into the stability of in-phase synchronized states, i.e., $\phi_i = \Omega t$, $i = 1, ..., N$. Note that the in-phase synchronized states belong to the class of antipodal states (see Section 3) and share the same dynamical properties [69,87]. We assume that the network topology expressed by the adjacency matrix possesses a constant row sum r, i.e., $r = \sum_{j=1}^{N} a_{ij}$ for all i. Following the master stability approach for networks with adaptive coupling weights as developed in [60], the master stability function is derived for networks of adaptively coupled phase oscillators. This can facilitate the separation of the effects of the local node dynamics from the effects of adaptivity as well as the network topology. Therefore, general conclusions on the stability of the in-phase synchronized state can be drawn for almost arbitrary complex network topologies. Accordingly, the master stability approach allows studying the interplay of nodal dynamics, adaptivity, and complex network structures. The approach, further, enables us to control the stability of the synchronized states, depending on the changes to the coupling structure. In the following, a brief discussion of the master stability function is provided for the adaptive Kuramoto-Sakaguchi network (1)–(2). Based on the results obtained from [60], the stability of the synchronous state of System (1)–(2) is governed by two linearized differential equations for perturbations of the synchronous state in the new coordinates $\zeta \in \mathbb{R}$ and $\kappa \in \mathbb{R}$:

$$\frac{d}{dt}\begin{pmatrix}\zeta\\ \kappa\end{pmatrix} = \begin{pmatrix}\mu\sigma\cos(\alpha)\sin(\beta) & -\sigma\sin(\alpha)\\ -\epsilon\mu\cos(\beta) & -\epsilon\end{pmatrix}\begin{pmatrix}\zeta\\ \kappa\end{pmatrix}, \quad (6)$$

where $\mu \in \mathbb{C}$ denotes all eigenvalues of the Laplacian matrix $L = r\mathbb{I}_N - A$ corresponding to the network described by the adjacency matrix A. Here, $\mathbb{I}_N$ is the N-dimensional identity matrix. The characteristic polynomial in λ of Eq. (6) is of second degree and reads:

$$\lambda^2 + (\epsilon - \sigma\mu\cos(\alpha)\sin(\beta))\lambda - \epsilon\sigma\mu\sin(\alpha+\beta) = 0. \quad (7)$$

The master stability function is given by $\Lambda(\sigma\mu) = \max(\mathrm{Re}(\lambda_1), \mathrm{Re}(\lambda_2))$ where λ_1 and λ_2 are the two solutions of the quadratic polynomial (7). Through the master stability function, the local stability of the in-phase state (also for the antipodal states) can be directly obtained from the connectivity structure given by the adjacency matrix. In particular, if there exists at least one Laplacian eigenvalue such that $\Lambda(\sigma\mu) > 0$, the state is locally unstable. If $\Lambda(\sigma\mu) < 0$ holds for all Laplacian eigenvalues, the in-phase synchronous state is locally stable. Note that with the construction of the Laplacian matrix L, there exists always one eigenvalue $\mu = 0$ which leads to $\lambda_1 = 0$ and $\lambda_2 = -\epsilon$. The zero eigenvalue of the matrix in (6) corresponds to the phase-shift symmetry of System (1)–(2) and it is not considered in the above stability condition.

In order to get an insight into the form of the master stability function, we consider the boundary of the region in $\sigma\mu$ parameter space that corresponds to stable local dynamics. The boundary is given by $\lambda = i\gamma$ with $\gamma \in \mathbb{R}$. Plugging this into Eq. (7), we obtain the function:

$$\sigma\mu = a(\gamma) + ib(\gamma),$$

with:

$$a(\gamma) = \epsilon\frac{\gamma^2(\cos\alpha\sin\beta - \sin(\alpha+\beta))}{\gamma^2\cos^2\alpha\sin^2\beta + \epsilon^2\sin^2(\alpha+\beta)},$$

$$b(\gamma) = \frac{\gamma^3\cos\alpha\sin\beta + \epsilon^2\gamma\sin(\alpha+\beta)}{\gamma^2\cos^2\alpha\sin^2\beta + \epsilon^2\sin^2(\alpha+\beta)}.$$

Hence, the boundary in the complex $\sigma\mu$-plane is parametrically defined as a cubic function of the real value γ. Due to the symmetry of the master stability function, a condition is required to observe a nontrivial shape of the boundary; in other words, function $\sigma\mu(\gamma)$ possesses three crossings with the real axis, i.e., two positive real solutions for $b(\gamma) = 0$. The three crossings are given by $\gamma_1 = 0$ and the real solutions γ_2 and γ_3 of $\gamma^2\cos\alpha\sin\beta = -\epsilon^2\ sin(\alpha+\beta)$. Given this, the existence condition for three crossings as $\sin(\alpha+\beta)/(\cos\alpha\sin\beta) < 0 (\epsilon > 0)$ can be obtained. Note that $a(\gamma_2) = a(\gamma_3)$. In case there are three crossings, the master stability function possesses a stability island in the complex plane. The following section focuses on the phenomenon induced by the existence of a stability island.

6. Destabilization of synchrony by changes in network connectivity

The emergence of stability islands in the master stability function enables us to destabilize synchronous states in different ways. In the following, desynchronization is demonstrated by modifying the network topology. A similar approach was studied on non-adaptive delay-coupled systems in [50,52]. As shown, randomly added inhibitory links contribute to the desynchronization transition on regular ring topologies. Then, random network topologies were employed to extend these studies to adaptively coupled systems.

This study takes into account a network of adaptively coupled phase oscillators, described by the set of differential equations (Eq. (1) and (2)). The oscillators are assumed to have a natural frequency $\omega = 1$. In the following, the stability of phase-synchronized states on networks with random adjacency matrices is investigated first using the master stability function and second, through numerical integration. The parameters α and β should be chosen to ensure a stability island for the master stability function in a complex plane. Then, random initial conditions should be prepared, i.e., $\phi_i(0) \in [0, 2\pi)$ and $\kappa_{ij}(0) \in [-1, 1]$ as well as the numerically integrated equations (Eq. (1) and (2)) with $N = 100$ and $t = 30000$ for three different random adjacency matrices, corresponding to the directed, connected networks with different node in-degrees. In order to guarantee the existence of the synchronized states, we assume that the adjacency matrices have a constant row sum $r = \sum_{j=1}^{N} a_{ij}$. Note that this condition is not preserved by the dilution procedure used in Section 3. The following procedure is then applied to construct the directed random networks. For each node i of the N nodes, r links are randomly picked from the set that consists of all possible links from nodes $j \neq i$ to node i. For the selected links, a_{ij} is set to 1. This procedure yields a directed random network with N nodes and a constant row sum (in-degree) r. Of note, the row sum r defines the ratio of the deleted links $q = Q/(N(N-1)) = 1-r/(N-1)$, i.e., the degree of dilution.

Figure 7(a), (b), and (c) show the master stability function $\Lambda(\sigma\mu)$ for the parameters $\alpha = 0.48\pi$ and $\beta = 0.91\pi$, where the black dots indicate the scaled Laplacian eigenvalues $\sigma\mu_i$ of three random adjacency matrices with different row sums r. This function is employed to determine the stability of the in-phase synchronized state for the given coupling topology and show the corresponding numerical results below.

For sparse random networks with $r = 3$ ($q = 0.97$), the synchronous state is stable (see Figure 7(a), (d), (g), and (j)). The stability follows directly from the master stability function, since all values $\sigma\mu_i$ for all Laplacian eigenvalues lie within the stable region $\Lambda(\sigma\mu) < 0$ (blue), see Figure 7(a). In this case, all oscillators have the same mean frequency $\langle\dot{\phi}_j\rangle$ (see Figure 7(g)). Moreover, the oscillators ϕ_j either share the same phase $a_i \approx a$ or the antipodal phase $a_i \approx a + \pi$, indicating an antipodal-type cluster. In-phase synchronous states considered by the master stability function Λ belong to the class of antipodal states and share the same local stability properties [87]. In the case of increasing the number of links, e.g., to $r = 50$ ($q = 0.49$), some of the Laplacian eigenvalues move out of the stable region of the master stability function into the unstable region (yellow/red) in the complex plane. Consequently, the in-phase synchronized state is locally unstable (see Figure 7(b)). In this case, antipodal-type multiclusters emerge, where the oscillators within each cluster share a common frequency (Figure 7(h)) and have antipodal phase relations (Figure 7(e)). The phases within the two smallest clusters spread out due to the fact that the adjacency matrix restricted to the clusters does not necessarily have a constant row sum. In the case of an all-to-all coupled network with $r = 99$ ($q = 0$), the values $\sigma\mu_i$ are either located at 0 or 1 (see Figure 7(c)). Since the eigenvalues located at $\sigma\mu = 1$ lie in the unstable region, the in-phase synchronized state is unstable. In this case, the emergence of an antipodal-type multicluster is observed again (see Figure 7(f), (i), and (l)).

This section discusses the effects induced by changes in the network topology on the desynchronization of the phase-synchronized state. While the phase-synchronized state is stable for sparse networks, it is destabilized for an increasing number of links. We have described this behavior by means of the master stability function for networks with adaptive coupling weights. Modifying the adjacency matrix affects the Laplacian eigenvalues μ_i and consequently, changes the largest Lyapunov exponents of the network. We use the presence of bounded stable regions (stability islands in the complex plane) of the master stability function to successively shift the Laplacian eigenvalues from the stable into the unstable regime by changing the network connectivity. We show that the resulting desynchronization has strong implications for the emergence of multicluster states.

7. Discussion

In the previous sections, we have investigated the emergence of cluster synchronization on networks of adaptively coupled Kuramoto-Sakaguchi oscillators with complex topologies. Specifically, we have focused on the robustness of the multifrequency cluster states against diluted connectivities. We have demonstrated the influence of topological changes on these states. Further, we have complemented these studies by an analytical approach describing the stability of phase-synchronized states. Investigating the master stability function for adaptive Kuramoto-Sakaguchi networks allowed us to study the interplay among nodal dynamics, adaptivity, and network topology. Accordingly, it was illustrated that the existence of adaptive coupling weights might dramatically change the synchronization behavior with regard to network topology.

In Section 3, previous findings on the emergence of multi-frequency-clusters on networks of adaptively coupled phase oscillators were reviewed and a notation describing the generic appearance of cluster states was introduced. It was numerically illustrated for all-to-all coupled networks that starting from random initial

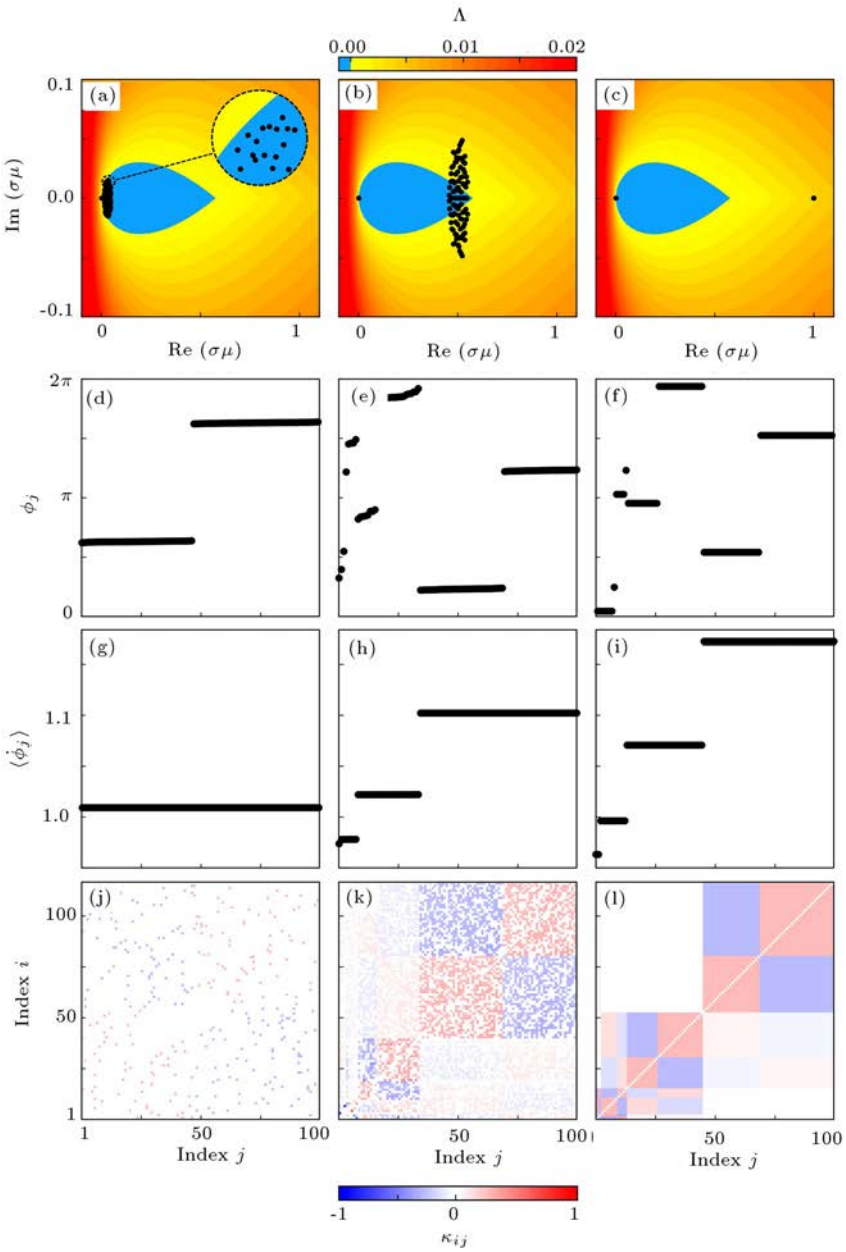

Figure 7. The interplay between network dynamics and topology. Dynamics in a network of $N = 100$ adaptively coupled phase oscillators (Eqs. (1) and (2)) with random adjacency matrices with different constant row sums $r = \sum_{j=1}^{N} a_{ij}$, and random initial conditions $\phi_i(0) \in [0, 2\pi\}$ and $\kappa_{ij}(0) \in [-1, 1]$ for $i, j = 1, ..., N$. The simulations results are shown for the three values ((a), (d), (g), and (j)) $r = 3$, ((b), (e), (h), and (k)) $r = 50$, and ((c), (f), (i), and (l)) $r = 99$. The panels show: ((a), (b), and (c)) The master stability function color coded together with $\sigma\mu_i$, where μ_i denotes the N Laplacian eigenvalues corresponding to each adjacency matrix; the inset in (a) depicts a blow-up of the marked area, where eigenvalues lie close to the border of the stability island; (d), (e), and (f) show the snapshots of the oscillator phases ϕ_j at $t = 30000$; (g), (h), and (i) present the mean frequencies $\langle\dot{\phi}_j\rangle = (\phi_j(t_0 + T) - \phi_j(t_0))/T$, where $t_0 = 25000$ and $T = 5000$; (j), (k), and (l) show the snapshots of the coupling weights κ_{ij}, where the coupling weights are color coded. The oscillators are ordered according to their mean frequencies $\langle\dot{\phi}_j\rangle$ and subsequently, their phases ϕ_j. Other parameters are $\alpha = 0.48\pi$, $\beta = 0.91\pi$, $\omega = 1$, $\sigma = 1/N$, and $\epsilon = 0.01$.

conditions, these systems could reach different types of multicluster states such as splay- and antipodal-type multiclusters. These states have previously been studied on all-to-all coupled networks [63,69,87], nonlocally coupled rings [89], multiplex [46,85], and random networks [88] with adaptive coupling weights. We extended these studies towards randomly diluted coupling topologies. In order to investigate the influence of topological changes upon these states, the adjacency matrix describing the underlying time-independent

coupling topology was modified. For this purpose, random adjacency matrices, representing directed random network topologies with varying degrees of dilution, were constructed.

As was shown in Section 4, the emergence of partially synchronized states was maintained on random networks with a small number of links. The emergence of different types of multicluster states including splay-type multiclusters was observed on densely coupled networks ($q = 0.13$ in Figure 4(c)). This result is in agreement with the findings presented in [88], where the dynamical states on networks of adaptively coupled phase oscillators were studied in the (α, β) parameter space for different network sparsity. Based on the numerical investigations, the multicluster states observed were multistable with regard to initial conditions, meaning that different multiclusters might emerge in different initial conditions. By depicting asymptotic states with different values of the ratio of deleted links q, it was illustrated that the qualitative shape of a given multicluster state was preserved on networks of different degrees of dilution. The number of clusters remains the same for a wide range of q; however, the frequencies of the oscillators adapt to the changes in the coupling topology in a linear relation with q. The latter effect has been analytically described.

Since in-phase synchronous and antipodal states have the same local stability properties, we have extended our investigations by an analytical approach describing the stability of in-phase synchronized states in Section 5. The master stability function for networks of Kuramoto-Sakaguchi oscillators with adaptive coupling weights was analyzed using novel methods presented in [60]. The emergence of bounded regions was observed which would lead to stable synchronous dynamics in the master stability function, representing stability islands in the complex plane. We analytically described the stability border and provided a condition for the emergence of stability islands. Due to the shape of these stability islands, it is possible to destabilize in-phase synchronized states by increasing the number of links within the network. Therefore, such destabilization had implications for the emergence of multicluster states. Upon tailoring the system configurations such that a stability island would emerge in the master stability function, we observed stable multicluster states emerging from random initial conditions for those topological configurations with unstable in-phase synchronized states. In the previous work [60], it was shown that such a counterintuitive desynchronization effect was also possible as the overall coupling strength increased.

8. Conclusion

The present study managed to show the emergence of multi-cluster states on networks of adaptively coupled Kuramoto-Sakaguchi oscillators with random coupling topologies. Owing to the adaptivity of the coupling weights, the individual oscillators could adapt their frequencies and form strongly coupled groups of frequency-synchronized units. In addition, numerical and analytical investigations revealed how random coupling topologies could affect the emergence of these synchronization patterns. While the structural shape of multi-clusters remained the same, the overall synchrony in a network declined by decreasing the number of links since more and more oscillators would decouple from the system and exhibit incoherent dynamics. Nonetheless, this study showed that by means of the master stability function, some network configurations allowed for stable in-phase synchronized dynamics for very sparse random networks. While our investigations were restricted to networks with uniform degree distributions, they might be generalized to more realistic network models such as small-world or scale-free networks. The master stability approach served as a universal tool, describing the stability of in-phase synchronized states. It was demonstrated that the destabilization of fully synchronized states had implications for the emergence of multicluster states. In order to obtain a more complete picture, this approach may be extended to splay-type synchrony. Our findings on the effects of diluted connectivity upon multicluster states illustrated the complex interplay between topology and adaptivity. By applying the master stability approach, it was clarified that the adaptive properties of a network could have a huge impact on the stability of fully and partially synchronized states since the presence of adaptivity provided a feedback mechanism that could change the stability; intuitively, this is similar to an additional effective phase lag.

Acknowledgments

This work was supported by the German Research Foundation DFG, Project Nos. 411803875 and 440145547.

References

1. Newman, M.E.J. "The structure and function of complex networks", *SIAM Review*, **45**(2), pp. 167–256 (2003).
2. Boccaletti, S., Pisarchik, A.N., del Genio, C.I., and Amann, A., *Synchronization: From Coupled Systems to Complex Networks*, Cambridge: Cambridge University Press (2018).
3. Pecora, L.M., Carroll, T.L., Johnson, G.A., Mar, D.J., and Heagy, J.F. "Fundamentals of synchronization in chaotic systems, concepts, and applications", *Chaos*, **7**(4), pp. 520–543 (1997).

4. Pikovsky, A., Rosenblum, M., and Kurths, J., *Synchronization: A Universal Concept in Nonlinear Sciences*, Cambridge: Cambridge University Press, 1st edition (2001).
5. Strogatz, S.H. "Exploring complex networks", *Nature*, **410**, pp. 268–276 (2001).
6. Yanchuk, S., Maistrenko, Y., and Mosekilde, E. "Synchronization of time-continuous chaotic oscillators", *Chaos*, **13**(1), pp. 388–400 (2003).
7. Arenas, A., Díaz-Guilera, A., Kurths, J., Moreno, Y., and Zhou, C. "Synchronization in complex networks", *Phys. Rep.*, **469**(3), pp. 93–153 (2008).
8. Huygens, C., *Horologium Oscillatorium: Sive de Motu Pendulorum Ad Horologia Aptato Demonstrationes Geometricae*, Christiaan Huygens, 1st edition (1673).
9. Kuramoto, Y., *Chemical Oscillations, Waves and Turbulence*, Berlin: Springer-Verlag (1984).
10. Dai, X., Li, X., Guo, H., Jia, D., Perc, M., Manshour, P., Wang, Z., and Boccaletti, S. "Discontinuous transitions and rhythmic states in the D-dimensional Kuramoto model induced by a positive feedback with the global order parameter", *Phys. Rev. Lett.*, **125**(19), p. 194101 (2020).
11. Yanchuk, S., Maistrenko, Y., and Mosekilde, E. "Partial synchronization and clustering in a system of diffusively coupled chaotic oscillators", *Math. Comp. Simul.*, **54**, pp. 491–508 (2001).
12. Sorrentino, F. and Ott, E. "Network synchronization of groups", *Phys. Rev. E*, **76**(5), p. 056114 (2007).
13. Dahms, T., Lehnert, J., and Schöll, E. "Cluster and group synchronization in delay-coupled networks", *Phys. Rev. E*, **86**(1), p. 016202 (2012).
14. Miyakawa, K., Okano, T., and Yamazaki, T. "Cluster synchronization in a chemical oscillator network with adaptive coupling", *Journal of the Physical Society of Japan*, **82**(3), p. 034005 (2013).
15. Zhang, Y. and Motter, A.E. "Symmetry-independent stability analysis of synchronization patterns", *SIAM Rev.*, **62**(4), pp. 817–836 (2020).
16. Kuramoto, Y. and Battogtokh, D. "Coexistence of coherence and incoherence in nonlocally coupled phase oscillators", *Nonlin. Phen. in Complex Sys.*, **5**(4), pp. 380–385 (2002).
17. Abrams, D.M. and Strogatz, S.H. "Chimera states for coupled oscillators", *Phys. Rev. Lett.*, **93**(17), p. 174102 (2004).
18. Motter, A.E. "Nonlinear dynamics: Spontaneous synchrony breaking", *Nat. Phys.*, **6**(3), pp. 164–165 (2010).
19. Panaggio, M.J. and Abrams, D.M. "Chimera states: Coexistence of coherence and incoherence in networks of coupled oscillators", *Nonlinearity*, **28**, p. R67 (2015).
20. Schöll, E. "Synchronization patterns and chimera states in complex networks: interplay of topology and dynamics", *Eur. Phys. J. Spec. Top.*, **225**, pp. 891–919 (2016).
21. Sawicki, J., Omelchenko, I., Zakharova, A., and Schöll, E. "Delay controls chimera relay synchronization in multiplex networks", *Phys. Rev. E*, **98**, p. 062224 (2018).
22. Omel'chenko, O.E. and Knobloch, E. "Chimerapedia: coherence-incoherence patterns in one, two and three dimensions", *New J. Phys.*, **21**(9), p. 093034 (2019).
23. Andrzejak, R.G., Ruzzene, G., Schöll, E., and Omelchenko, I. "Two populations of coupled quadratic maps exhibit a plentitude of symmetric and symmetry broken dynamics", *Chaos*, **30**(3), p. 033125 (2020).
24. Drauschke, F., Sawicki, J., Berner, R., Omelchenko, I., and Schöll, E. "Effect of topology upon relay synchronization in triplex neuronal networks", *Chaos*, **30**, p. 051104 (2020).
25. Schöll, E., Zakharova, A., and Andrzejak, R.G., *Chimera States in Complex Networks. Research Topics, Front. Appl. Math. Stat.*, Lausanne: Frontiers Media SA (2020). Ebook.
26. Zakharova, A., *Chimera Patterns in Networks: Interplay between Dynamics, Structure, Noise, and Delay. Understanding Complex Systems*, Springer (2020).
27. Schöll, E. "Chimeras in physics and biology: Synchronization and desynchronization of rhythms", *Nova Acta Leopoldina*, **425**, pp. 67–95 (2020). Invited contribution.
28. Parastesh, F., Jafari, S., Azarnoush, H., Shahriari, Z., Wang, Z., Boccaletti, S., and Perc, M. "Chimeras", *Phys. Rep.*, **898**, pp. 1–114 (2021).
29. Singer, W. "Neuronal synchrony: A versatile code review for the definition of relations", *Neuron*, **24**, pp. 49–65 (1999).
30. Wang, X.J. "Neurophysiological and computational principles of cortical rhythms in cognition", *Phys. Rev.*, **90**(3), pp. 1195–1268 (2010).
31. Fell, J. and Axmacher, N. "The role of phase synchronization in memory processes", *Nat. Rev. Neurosci.*, **12**(2), pp. 105–118 (2011).
32. Hammond, C., Bergman, H., and Brown, P. "Pathological synchronization in Parkinson's disease: networks, models and treatments", *Trends Neurosci.*, **30**, pp. 357–364 (2007).
33. Schiff, S.J. "Towards model-based control of Parkinson's disease", *Phil. Trans. R. Soc. A*, **368**, pp. 2269–2308 (2010).
34. Kromer, J.A. and Tass, P.A. "Long-lasting desynchronization by decoupling stimulation", *Phys. Rev. Research*, **2**(3), p. 033101 (2020).
35. Kromer, J.A., Khaledi-Nasab, A., and Tass, P.A. "Impact of number of stimulation sites on long-lasting desynchronization effects of coordinated reset stimulation", *Chaos*, **30**(8), p. 083134 (2020).

36. Lehnertz, K., Bialonski, S., Horstmann, M.T., Krug, D., Rothkegel, A., Staniek, M., and Wagner, T. "Synchronization phenomena in human epileptic brain networks", *J. Neurosci. Methods*, **183**(1), pp. 42–48 (2009).

37. Mormann, F., Lehnertz, K., David, P., and Elger, C.E. "Mean phase coherence as a measure for phase synchronization and its application to the EEG of epilepsy patients", *Physica D*, **144**(3–4), pp. 358–369 (2000).

38. Jiruska, P., de Curtis, M., Jefferys, J.G.R., Schevon, C.A., Schiff, S.J., and Schindler, K. "Synchronization and desynchronization in epilepsy: controversies and hypotheses", *J. Physiol.*, **591**(4), pp. 787–797 (2013).

39. Jirsa, V.K., Stacey, W.C., Quilichini, P.P., Ivanov, A.I., and Bernard, C. "On the nature of seizure dynamics", *Brain*, **137**, p. 2210 (2014).

40. Rothkegel, A. and Lehnertz, K. "Irregular macroscopic dynamics due to chimera states in small-world networks of pulse-coupled oscillators", *New J. Phys.*, **16**, p. 055006 (2014).

41. Andrzejak, R.G., Rummel, C., Mormann, F., and Schindler, K. "All together now: Analogies between chimera state collapses and epileptic seizures", *Sci. Rep.*, **6**, p. 23000 (2016).

42. Chouzouris, T., Omelchenko, I., Zakharova, A., Hlinka, J., Jiruska, P., and Schöll, E. "Chimera states in brain networks: empirical neural vs. modular fractal connectivity", *Chaos*, **28**(4), p. 045112 (2018).

43. Gerster, M., Berner, R., Sawicki, J., Zakharova, A., Skoch, A., Hlinka, J., Lehnertz, K., and Schöll, E. "FitzHugh-Nagumo oscillators on complex networks mimic epileptic-seizure-related synchronization phenomena", *Chaos*, **30**, p. 123130 (2020).

44. Pecora, L.M. and Carroll, T.L. "Master stability functions for synchronized coupled systems", *Phys. Rev. Lett.*, **80**(10), pp. 2109–2112 (1998).

45. Brechtel, A., Gramlich, P., Ritterskamp, D., Drossel, B., and Gross, T. "Master stability functions reveal diffusion-driven pattern formation in networks", *Phys. Rev. E*, **97**(3), p. 032307 (2018).

46. Berner, R., Sawicki, J., and Schöll, E. "Birth and stabilization of phase clusters by multiplexing of adaptive networks", *Phys. Rev. Lett.*, **124**(8), p. 088301 (2020).

47. Choe, C.U., Dahms, T., Hövel, P., and Schöll, E. "Controlling synchrony by delay coupling in networks: from in-phase to splay and cluster states", *Phys. Rev. E*, **81**(2), p. 025205(R) (2010).

48. Flunkert, V., Yanchuk, S., Dahms, T., and Schöll, E. "Synchronizing distant nodes: a universal classification of networks", *Phys. Rev. Lett.*, **105**, p. 254101 (2010).

49. Greenshields, C. "Master stability function for systems with two coupling delays", *Private Communication* (2010).

50. Lehnert, J., Dahms, T., Hövel, P., and Schöll, E. "Loss of synchronization in complex neural networks with delay", *Europhys. Lett.*, **96**, p. 60013 (2011).

51. Flunkert, V., Yanchuk, S., Dahms, T., and Schöll, E. "Synchronizability of networks with strongly delayed links: a universal classification", *Contemp. Math.*, **48**, pp. 134–148 (2013). English version: J. of Math. Sciences (Springer) (2014).

52. Keane, A., Dahms, T., Lehnert, J., Suryanarayana, S.A., Hövel, P., and Schöll, E. "Synchronisation in networks of delay-coupled type-I excitable systems", *Eur. Phys. J. B*, **85**(12), p. 407 (2012).

53. Wille, C., Lehnert, J., and Schöll, E. "Synchronization-desynchronization transitions in complex networks: An interplay of distributed time delay and inhibitory nodes", *Phys. Rev. E*, **90**, p. 032908 (2014).

54. Kyrychko, Y.N., Blyuss, K.B., and Schöll, E. "Synchronization of networks of oscillators with distributed-delay coupling", *Chaos*, **24**, p. 043117 (2014).

55. Lehnert, J. "Controlling synchronization patterns in complex networks", Springer Theses, Heidelberg: Springer (2016).

56. Huddy, S.R. and Sun, J. "Master stability islands for amplitude death in networks of delaycoupled oscillators", *Phys. Rev. E*, **93**, p. 052209 (2016).

57. Börner, R., Schultz, P., Unzelmann, B., Wang, D., Hellmann, F., and Kurths, J. "Delay master stability of inertial oscillator networks", *Phys. Rev. Research*, **2**(2), p. 023409 (2020).

58. Sorrentino, F. "Synchronization of hypernetworks of coupled dynamical systems", *New J. Phys.*, **14**, p. 033035 (2012).

59. Mulas, R., Kuehn, C., and Jost, J. "Coupled dynamics on hypergraphs: Master stability of steady states and synchronization", *Phys. Rev. E*, **101**(6), p. 062313 (2020).

60. Berner, R., Vock, S., Schöll, E., and Yanchuk, S. "Desynchronization transitions in adaptive networks", *Phys. Rev. Lett.*, **126**(2), p. 028301 (2021).

61. Gross, T. and Blasius, B. "Adaptive coevolutionary networks: a review", *J. R. Soc. Interface*, **5**(20), pp. 259–271 (2008).

62. Aoki, T. and Aoyagi, T. "Co-evolution of phases and connection strengths in a network of phase oscillators", *Phys. Rev. Lett.*, **102**, p. 034101 (2009).

63. Kasatkin, D.V., Yanchuk, S., Schöll, E., and Nekorkin, V.I. "Self-organized emergence of multi-layer structure and chimera states in dynamical networks with adaptive couplings", *Phys. Rev. E*, **96**(6), p. 062211 (2017).

64. Gerstner, W., Kempter, R., von Hemmen, J.L., and Wagner, H. "A neuronal learning rule for sub-

millisecond temporal coding", *Nature*, **383**(6595), pp. 76–78 (1996).

65. Abbott, L.F. and Nelson, S. "Synaptic plasticity: taming the beast", *Nat. Neurosci.*, **3**(11), pp. 1178–1183 (2000).

66. Dan, Y. and Poo, M.M. "Spike timing-dependent plasticity: from synapse to perception", *Physiol. Rev.*, **86**(3), pp. 1033–1048 (2006).

67. Clopath, C., Büsing, L., Vasilaki, E., and Gerstner, W. "Connectivity reflects coding: a model of voltage-based STDP with homeostasis", *Nat. Neurosci.*, **13**(3), pp. 344–352 (2010).

68. Seliger, P., Young, S.C., and Tsimring, L.S. "Plasticity and learning in a network of coupled phase oscillators", *Phys. Rev. E*, **65**(4), p. 041906 (2002).

69. Berner, R., Schöll, E., and Yanchuk, S. "Multiclusters in networks of adaptively coupled phase oscillators", *SIAM J. Appl. Dyn. Syst.*, **18**(4), pp. 2227–2266 (2019).

70. Sakaguchi, H. and Kuramoto, Y. "A soluble active rotater model showing phase transitions via mutual entertainment", *Prog. Theor. Phys*, **76**(3), pp. 576–581 (1986).

71. Asl, M.M., Valizadeh, A., and Tass, P.A. "Dendritic and axonal propagation delays may shape neuronal networks with plastic synapses", *Front. Physiol.*, **9**, p. 1849 (2018).

72. Daido, H. "Order function and macroscopic mutual entrainment in uniformly coupled limitcycle oscillators", *Prog. Theor. Phys.*, **88**(6), pp. 1213–1218 (1992).

73. Rodrigues, F.A., Peron, T.K.D.M., Ji, P., and Kurths, J. "The Kuramoto model in complex networks", *Phys. Rep.*, **610**, pp. 1–98 (2016).

74. Ren, Q. and Zhao, J. "Adaptive coupling and enhanced synchronization in coupled phase oscillators", *Phys. Rev. E*, **76**(1), p. 016207 (2007).

75. Aoki, T. and Aoyagi, T. "Self-organized network of phase oscillators coupled by activity dependent interactions", *Phys. Rev. E*, **84**, p. 066109 (2011).

76. Picallo, C.B. and Riecke, H. "Adaptive oscillator networks with conserved overall coupling: Sequential firing and near-synchronized states", *Phys. Rev. E*, **83**(3), p. 036206 (2011).

77. Ha, S.Y., Noh, S.E., and Park, J. "Synchronization of Kuramoto oscillators with adaptive couplings", *SIAM J. Appl. Dyn. Syst.*, **15**(1), pp. 162–194 (2016).

78. Avalos-Gaytán, V., Almendral, J.A., Leyva, I., Battiston, F., Nicosia, V., Latora, V., and Boccaletti, S. "Emergent explosive synchronization in adaptive complex networks", *Phys. Rev. E*, **97**(4), p. 042301 (2018).

79. Maistrenko, Y., Lysyansky, B., Hauptmann, C., Burylko, O., and Tass, P.A. "Multistability in the Kuramoto model with synaptic plasticity", *Phys. Rev. E*, **75**(6), p. 066207 (2007).

80. Kasatkin, D.V. and Nekorkin, V.I. "Dynamics of the phase oscillators with plastic couplings", *Radiophysics and Quantum Electronics*, **58**(11), pp. 877–891 (2016).

81. Nekorkin, V.I. and Kasatkin, D.V. "Dynamics of a network of phase oscillators with plastic couplings", *AIP Conf. Proc.*, **1738**(1), p. 210010 (2016).

82. Aoki, T. and Aoyagi, T. "Scale-free structures emerging from co-evolution of a network and the distribution of a diffusive resource on it", *Phys. Rev. Lett.*, **109**(20), p. 208702 (2012).

83. Gushchin, A., Mallada, E., and Tang, A. "Synchronization of phase-coupled oscillators with plastic coupling strength", In *Information Theory and Applications Workshop ITA 2015*, San Diego, CA, USA, pp. 291–300, IEEE (2015).

84. Timms, L. and English, L.Q. "Synchronization in phase-coupled Kuramoto oscillator networks with axonal delay and synaptic plasticity", *Phys. Rev. E*, **89**(3), p. 032906 (2014).

85. Kasatkin, D.V. and Nekorkin, V.I. "Synchronization of chimera states in a multiplex system of phase oscillators with adaptive couplings", *Chaos*, **28**, p. 093115 (2018).

86. Kachhvah, A.D., Dai, X., Boccaletti, S., and Jalan, S. "Interlayer Hebbian plasticity induces first-order transition in multiplex networks", *New J. Phys.*, **22**, p. 122001 (2020).

87. Berner, R., Fialkowski, J., Kasatkin, D.V., Nekorkin, V.I., Yanchuk, S., and Schöll, E. "Hierarchical frequency clusters in adaptive networks of phase oscillators", *Chaos*, **29**(10), p. 103134 (2019).

88. Kasatkin, D.V. and Nekorkin, V.I. "The effect of topology on organization of synchronous behavior in dynamical networks with adaptive couplings", *Eur. Phys. J. Spec. Top.*, **227**, p. 1051 (2018).

89. Berner, R., Polanska, A., Schöll, E., and Yanchuk, S. "Solitary states in adaptive nonlocal oscillator networks", *Eur. Phys. J. Spec. Top.*, **229**(12–13), pp. 2183–2203 (2020).

Appendix

Figure 4(b) and (c) indicate that system (1)–(2) is multistable with regard to initial conditions. In other words, depending upon the initial state, different realizations of multicluster states can emerge. As shown in Figure A.1, the coupling matrices κ_{ij} are given at different values of q. Note that the presented coupling matrices correspond to the dynamics shown in Figure 5(II).

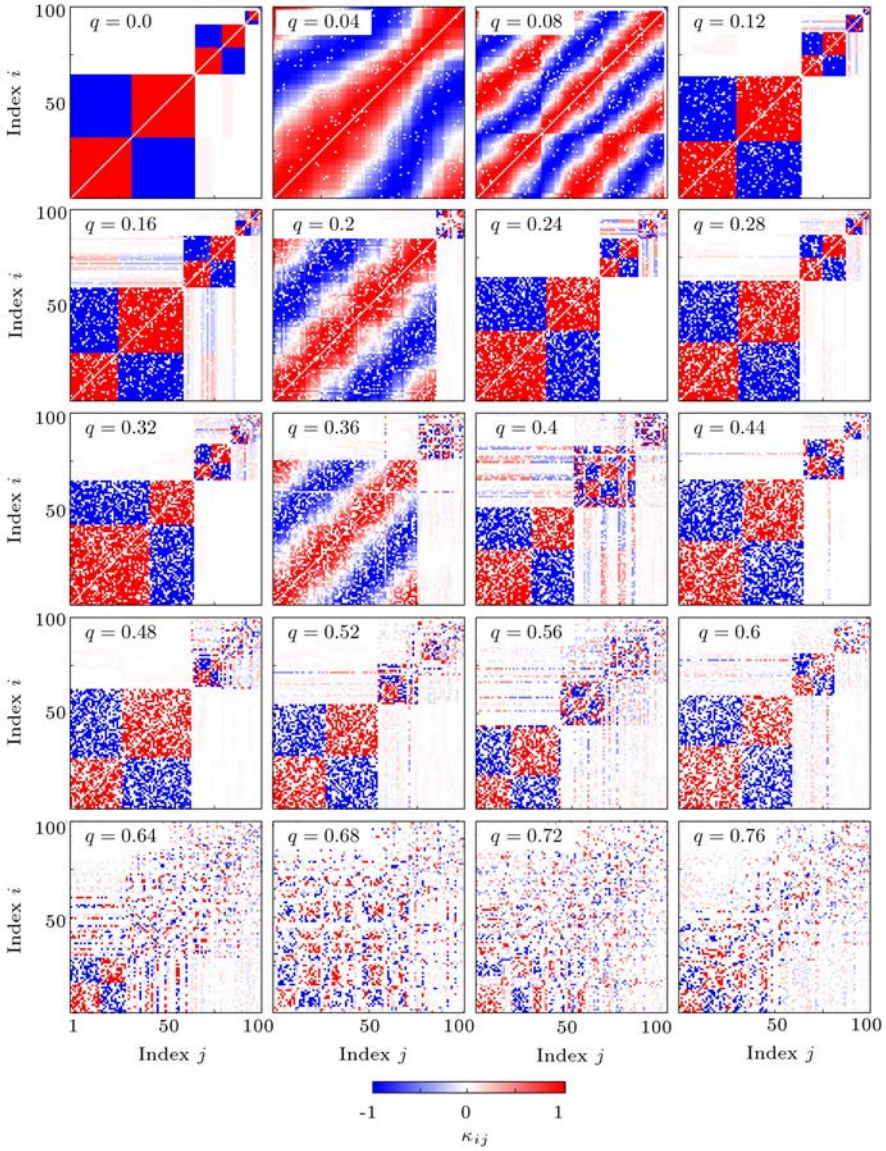

Figure A.1. Multicluster states in a network of adaptivley coupled phase oscillators (Eqs. (1) and (2)) with an increasing ratio of randomly deleted links q and random initial conditions. Snapshots of the coupling matrices κ_{ij} at $t = 11000$ for different values of q are presented. In each panel, the oscillators are ordered according to their average frequency and subsequently the phases. Parameters are $\alpha = 0.3\pi$, $\beta = -0.53\pi$, $\omega = 1$, $\epsilon = 0.01$, $N = 100$.

Biographies

Simon Vock studied Physics at TU Berlin, where he received the MSc degree in 2020. His research interests include synchronization, nonlinear dynamical systems, adaptive networks, and multi-cluster states.

Rico Berner studied Physics and Mathematics at TU Berlin, where he received his Dr. rer. nat. degree in 2020. He has worked with Siemens AG on applications of machine learning algorithms and has been the coordinator of school activities at Matheon (TU Berlin). His research interests include the analysis of nonlinear dynamical systems, synchronization phenomena in complex networks, and modeling of neuronal and technological systems.

Serhiy Yanchuk studied Theoretical Physics at the Moscow Engineering Physics Institute (Technical University) and received his PhD and DSc from the Academy of Sciences of Ukraine in 1997 and 2010, respectively. He worked as a senior researcher at the Institute of Mathematics, Ukrainian Academy of Sciences, a postdoctoral fellow at the Weierstrass Institute, Berlin, Junior Research Group Leader at Humboldt University Berlin. He was the Visiting Professor at Technical University of Berlin, Humboldt University of Berlin and Institute for Cross-

Disciplinary Physics and Complex Systems (Palma, Spain). His research primarily focuses on nonlinear dynamics including dynamical networks, spatio-temporal behavior of distributed systems, systems with time delays, and applications to neuronal, optoelectronic, machine learning, and other systems.

Eckehard Schöll is a Professor of Theoretical Physics at Technische Universität Berlin, Germany, a Principal Investigator of Bernstein Center for Computational Neuroscience Berlin, and a Guest Scientist at Potsdam Institute for Climate Impact Research. He is also the President of the International Physics and Control Society (IPACS). He studied Physics at University of Tübingen (Diplom 1976). He holds PhD degrees in Mathematics from the University of Southampton (UK, 1978) and Physics from RWTH Aachen (Germany, 1981). He also received his Honorary Doctorate from Saratov State University, Russia in 2017. As an expert in the field of nonlinear dynamics in complex systems and networks, he is also the head of the group of Nonlinear Dynamics and Control. He has worked on self-organized spatio-temporal pattern formation and its control, for instance, using time-delayed feedback methods, stochastic influences and noise, and semiconductor optoelectronics. His latest research is also related to topics in biology and energy systems, e.g., simulation of the dynamics in neuronal networks and power grids, synchronization patterns in complex networks and the interplay between nonlinear dynamics, network topology, and coupling delay. He is one of the forerunners of the study of chimera states.